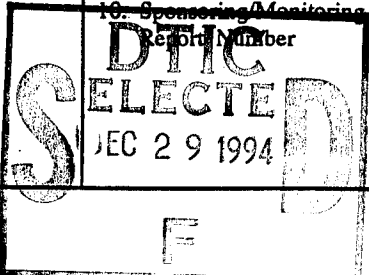


Report Documentation Page

1. Agency Use Only (Leave Blank)		2. Report Date Dec. 20, 1994	3. Report Type and Dates Covered Interim Technical	
4. Title and Subtitle Boron-induced Morphology Changes in Silicon CVD Growth: A Scanning Tunneling Microscopy Study			5. Funding Numbers N00014-91-J-1629 R&T Code 413S001	
6. Author(s) Robert J. Hamers and Yajun Wang				
7. Performing Organization Name(s) and Address(es) University of Wisconsin-Madison Dept. of Chemistry 1101 University Avenue Madison, WI 53706			8. Performing Organization Reprt Number #24	
9. Sponsoring/Monitoring Agency Name(s) and Address(es) U.S. Office of Naval Research Solid State and Surface Chemistry Program 1101 N. Quincy St. Arlington, VA 22217-5000			10. Sponsoring/Monitoring Agency Report Number  DTIC SELECTED DEC 29 1994	
11. Supplementary Notes Prepared for publication in Applied Physics Letters				
12a. Distribution/Availability Statement Approved for public release; distribution unlimited		12b. Distribution Code		
13. Abstract (Maximum 200 words) <p>Scanning tunneling microscopy has been used to investigate the influence of surface boron on silicon growth via chemical vapor deposition (CVD). The presence of boron-induced reconstructions on the Si(001) surface dramatically changes the surface morphology during subsequent CVD growth of silicon using disilane at 815 Kelvin. Boron-induced reconstructions inhibit the lateral diffusion of silicon atoms from terraces to step edges, leading to greatly enhanced island nucleation, and also reduce the local surface reactivity toward disilane. Strong segregation of boron to the growth surface allows the enhanced island nucleation to persist to subsequent terraces during multilayer CVD growth of silicon, producing a rough but epitaxial surface.</p> <p>19941227 087</p> <p>DTIC QUALITY INSPECTED 2</p>				
14. Subject Terms			15. Number of Pages' 12	
			16. Price Code	
17. Security Classification of Report Unclassified	18. Security Classification of this Page Unclassified	19. Security Classification of Abstract Unclassified	20. Limitation of Abstract UL	

U.S. OFFICE OF NAVAL RESEARCH

GRANT N00014-91-J-1629

R&T Code 413S001

Technical Report #24

**Boron-induced Morphology Changes in Silicon CVD Growth:
A Scanning Tunneling Microscopy Study**

by

Y. Wang and R.J. Hamers

Prepared for Publication

in

Applied Physics Letters

Dec. 20, 1994

Department of Chemistry
University of Wisconsin-Madison
Madison, WI 53706

Reproduction in whole or in part is permitted for any purpose of the United States Government.

This document has been approved for public release and sale: its distribution is unlimited.

Boron-induced Morphology Changes in Silicon CVD Growth: A Scanning Tunneling Microscopy Study

Yajun Wang and Robert J. Hamers*

Department of Chemistry

University of Wisconsin

1101 University Avenue

Madison, WI 53706

Abstract:

Scanning tunneling microscopy has been used to investigate the influence of surface boron on silicon growth via chemical vapor deposition (CVD). The presence of boron-induced reconstructions on the Si(001) surface dramatically changes the surface morphology during subsequent CVD growth of silicon using disilane at 815 Kelvin. Boron-induced reconstructions inhibit the lateral diffusion of silicon atoms from terraces to step edges, leading to greatly enhanced island nucleation, and also reduce the local surface reactivity toward disilane. Strong segregation of boron to the growth surface allows the enhanced island nucleation to persist to subsequent terraces during multilayer CVD growth of silicon, producing a rough but epitaxial surface.

*Author to whom correspondence should be addressed

Accession For	
NTIS CRA&I	<input checked="" type="checkbox"/>
DTIC TAB	<input type="checkbox"/>
Unannounced	<input type="checkbox"/>
Justification	
By	
Distribution /	
Availability Codes	
Dist	Avail and/or Special
A-1	

Dopants play an important role in chemical vapor deposition (CVD) processes not only by modifying the electrical properties of semiconductors, but also by influencing the growth rate and growth morphology of the resulting films.¹⁻¹⁰ Recent studies¹¹⁻¹⁶ have demonstrated the possibility of growing thin boron-doped Si layers in which the local boron concentration exceeds the bulk solubility limit by several orders of magnitude, motivating the need for an atomic-level understanding of the mechanisms by which dopants modify the chemical reactivity and morphology during growth.

In recent scanning tunneling microscopy studies^{17, 18} we showed that decomposition of diborane and/or decaborane on the Si(001) surfaces produces several ordered reconstructions and a strong lateral phase segregation of boron on the Si(001) surface. In this paper, we show how these boron-induced reconstructions affect the chemical reactivity and morphology of surfaces produced by subsequent chemical vapor deposition using disilane.

Samples of 0.01 ohm-cm, Sb-doped Si(001) wafers were cleaned by annealing to 1425 K in ultrahigh vacuum, producing large flat planes separated by monatomic steps. As shown in fig. 1, upon exposure to diborane at 815 Kelvin, boron incorporates into the crystal lattice and produces several closely-related boron-induced reconstructions.^{17, 18} Fig. 1a shows that these ordered reconstructions are accompanied by a strong lateral segregation, such that the boron atoms are not uniformly distributed on the surface. Instead, the high-resolution in fig. 1b shows that the surface consists of regions of well-ordered $c(4 \times 4)$ symmetry and other regions of (2×1) symmetry which appear identical to the clean Si(001) surface. Surfaces of Si(001) exposed to boron-containing precursors at less than saturation exposure (3000 Langmuirs for diborane) are best described as domains of boron-rich $c(4 \times 4)$ mixed with domains of "clean" Si(001)- (2×1) , in proportions varying with the boron exposure.

Figure 2 directly compares CVD growth from disilane on the diborane-exposed (2a-2c) and clean Si(001) (2d) surfaces. In fig. 2a-2c, Si(001) surfaces were first exposed to diborane to produce phase-segregated regions of $c(4 \times 4)$ -B/Si(001) occupying <5% of the total surface area, leaving >95% of the initial surface as clean Si(001)- (2×1) . The diborane-exposed surfaces (2a-2c) and clean Si(001) surface (2d) were then exposed to 10% Si₂H₆/He at a pressure of 5×10^{-7} Torr (2a) or 2.5×10^{-6} Torr (2b-2d) at 815 Kelvin, resulting in growth of approximately 2 monolayers Si for fig. 2a and 10 monolayers Si for fig. 2b-2d.

After growth of two monolayers of Si on the boron-exposed surface, fig. 2a shows that the predominant growth mode is by island formation, while on a clean Si(001) surface (not shown) growth using the identical procedure produces almost entirely step-flow growth. The influence of boron on the growth morphology is even more dramatic after growth of 10 monolayers. Fig. 2b shows that growth of 10 layers of Si on the boron-exposed surface produces a rough surface. At higher resolution, fig. 2c shows that despite the surface roughness the Si growth is still crystalline and epitaxial, since dimer rows running along the substrate crystallographic directions can be easily observed. Fig. 2c also shows that the growth surface is decorated with regions exhibiting the same boron-induced reconstruction as the original substrate surface, as indicated by the arrows. Therefore, it can be concluded that during CVD growth some of the boron "floats" to the surface layer instead of being completely buried at the original interface. For comparison, fig. 2d shows a large-scale STM image

produced after identical CVD growth on an initially-clean Si(001) surface; here, we observe that growth occurs primarily by layer-by-layer growth, with only minimal formation of islands.

In an effort to quantify the boron surface segregation, the number of surface unit cells attributed to the boron-induced reconstruction was measured on several surfaces before and after growth of disilane. (Based on our previous work,^{17, 18} each unit cell contains four boron atoms). In fig. 2c, for example, the starting surface contained 3.9×10^{-2} unit cells/nm², while after growth of 10 monolayers of Si at a rate of 0.015 monolayer/second at 815 K, the topmost layer contained 1.4×10^{-2} unit cells/nm², indicating that 36% of the boron remains at the growth surface. Similar experiments under a variety of growth conditions show that the concentration of boron observed at the surface is too high to be explained by isotropic bulk diffusion and inconsistent with the 4 eV barrier for boron diffusion observed in bulk Si.¹⁹

In addition to the segregation at the surface, our data clearly show that boron initiates island formation, resulting in a significantly rougher surface than growth on the corresponding clean surface. Fig. 3a shows the surface height distribution for the images shown in fig. 2d and 2b. While growth on the clean surface is confined almost entirely to four atomic layers, growth on the boron-exposed surface extends to ten layers and shows a nearly Gaussian height distribution. This is quantified in fig. 3b, which shows the height-height correlation function^{20, 21} $G(r) \equiv \langle [h(\bar{r}_0) - h(\bar{r}_0 + \bar{r})]^2 \rangle$ for these two surfaces. A fit of $G(r)$ to the typical self-affine scaling model $G(r) \propto \exp(2\alpha r)$ leads to a roughness exponent of $\alpha = 0.55 \pm 0.01$ and a lateral correlation length $\xi = 200$ Å for the boron-exposed surface, compared with $\alpha = 0.29 \pm 0.01$ and a $\xi \geq 300$ Å for growth on the clean surface under identical conditions. Fig. 2b indicates that Si layers grown on the boron-exposed surfaces are self-affine on length scales of < 200 Å.

In order to better understand the mechanism by which surface boron initiates island growth, STM was used to investigate the relative chemical reactivities of the clean and boron-reconstructed regions toward disilane at 300 Kelvin. These experiments showed that the reactive sticking probability for disilane is much lower on the boron-reconstructed regions than on the clean Si(001) surface, indicating that the island formation does not arise from preferential sticking or dissociation of disilane at the boron sites. In addition, when the boron-induced reconstructions occupy only a small fraction of the surface area, the total amount of silicon deposited from disilane (and hence, the average CVD growth rate) is nearly the same as on the clean surface, indicating the *small* amounts of boron do not significantly affect the CVD growth rate, in agreement with a recent study by Bramblett, et al.⁴ A decreased CVD growth rate is expected when the B-induced reconstructions occupy a significant fraction of the surface.⁷ Attempts to identify the location of the initial island nuclei by studying the spatial distribution of islands relative to the boron-reconstructed regions were inconclusive due to the strong surface segregation and possibility of lateral diffusion of boron atoms.

The above results demonstrate that when the surface boron concentration is small, disilane adsorption and dissociation take place primarily on the clean regions of the surface. At 815 Kelvin the boron-induced reconstructions affect the surface morphology by restricting subsequent silicon diffusion from the terraces to the step edges, leading to a transition from step-flow to island growth. As the islands become larger and encroach

upon the boron-induced reconstructions of the substrate, the boron is able to quickly diffuse to the outermost surface layer, but does not diffuse toward the bulk. As a result of the boron segregation to the surface, the restriction of diffusion is not limited only to the first silicon layer, but also extends to subsequent silicon layers as well. This leads to inefficient incorporation of boron into the silicon as a dopant and also leads to a dramatically enhanced island density as subsequent layers are grown on the surface. The high island density formed on each layer during CVD growth in turn leads to a crystalline but comparatively rough surface, as demonstrated by the large value of the roughness exponent in fig. 3b. Previous studies of the influence of boron on crystal quality have been inconclusive, with some reporting improved crystalline quality^{2, 22} and others reporting decreased quality.^{3, 23} A full understanding of boron's effect on CVD will require a model incorporating the rates of surface segregation, bulk diffusion, island nucleation, and surface diffusion for both boron and silicon.

The strong surface segregation of boron indicates that the boron atoms have a lower free energy at the surface than in the bulk. Parry, et al.¹⁰ reported a similar surface enrichment of boron during CVD growth and calculated an activation barrier of 0.8 eV for diffusion to the exposed growth surface, compared with 4 eV for bulk diffusion of boron in Si.¹⁹ Weir, et al.¹⁵ found that at temperatures of less than 575 K crystalline Si could be grown on boron "delta-doped" layers without significant boron diffusion or segregation. Our results show that at the higher temperatures used for CVD growth (here, 815 Kelvin), when Si atoms cover the boron-induced reconstructions the B atoms can easily hop by one lattice constant to remain at the surface, and support a low activation barrier of <2 eV for this process. This suggests indicate that while CVD techniques can be used to deposit the boron using diborane as a precursor, the higher temperatures necessary for CVD compared with MBE also result in greatly enhanced boron surface segregation and likely preclude the use of CVD for growth of buried "delta-doped" layers in which the boron atoms are confined to only a few atomic layers.

This work was supported in part by the U.S. Office of Naval Research and the National Science Foundation Presidential Faculty Fellowship Program.

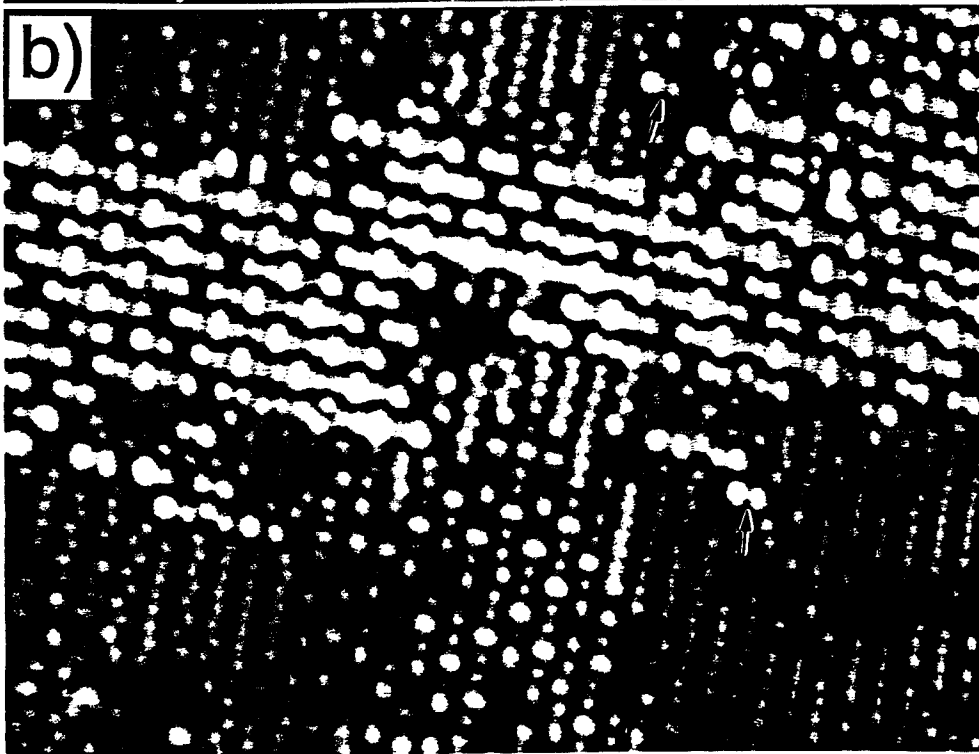
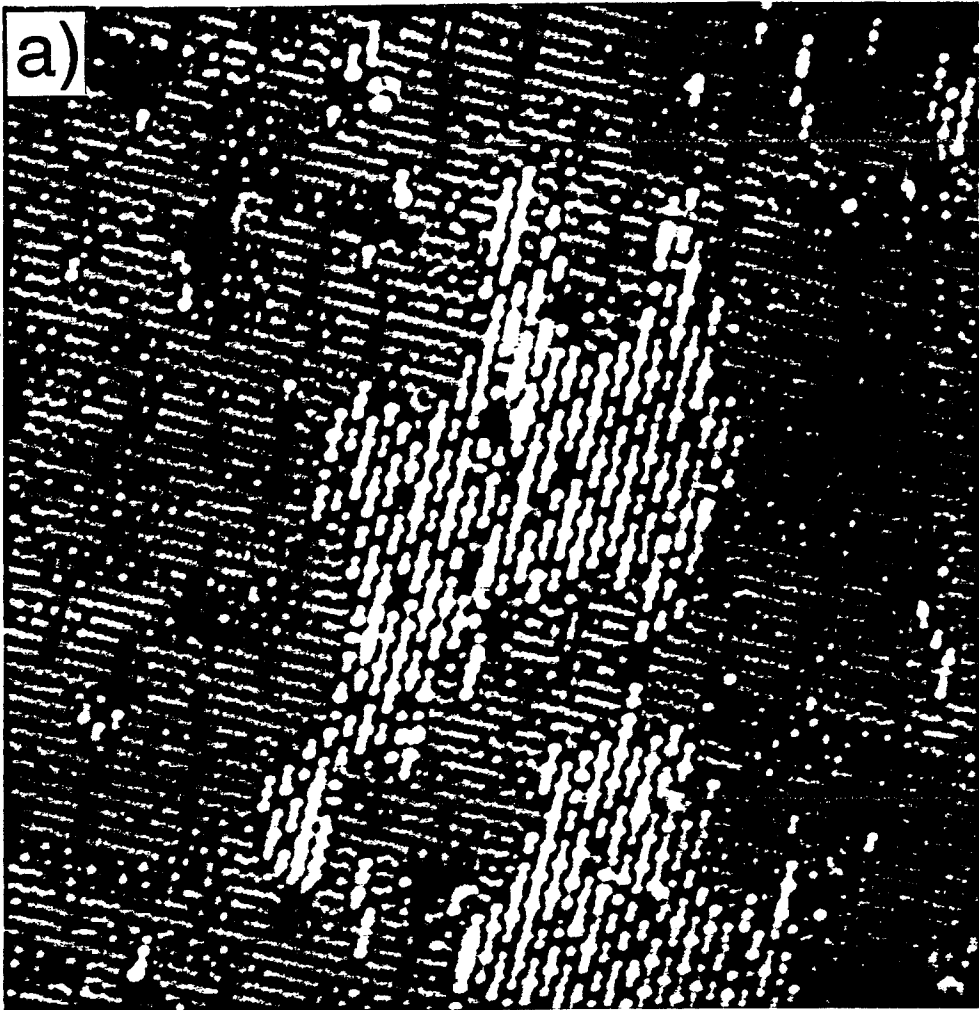
References:

- ¹C.-A. Chang and W.J. Siekhaus, *J. Appl. Phys.* **46**, 3402 (1975).
- ²T.Y. Hsieh, K.H. Jung, D.L. Kwong, Y.M. Kim and R. Brennan, *Appl. Phys. Lett.* **61**, 474 (1992).
- ³H.-C. Lin, H.-Y. Lin, C.-Y. Chang, T.-G. Jung, P.J. Wang, R.-C. Deng and J. Lin, *J. Appl. Phys.* **76**, 1572 (1994).
- ⁴T.R. Bramblett, Q. Lu, T. Karasawa, M.-A. Hasan, S.K. Jo and J.E. Greene, *J. Appl. Phys.* **76**, 1884 (1994).
- ⁵T.L. Lin, R.W. Fathauer and P.J. Grunthner, *Appl. Phys. Lett.* **55**, 795 (1989).
- ⁶H.-C. Lin, H.-Y. Lin, C.-Y. Chang, T.-F. Lei, P.J. Wang, R.-C. Deng, J. Lin and C.Y. Chao, *Appl. Phys. Lett.* **63**, 1525 (1993).
- ⁷R. Kircher, M. Furuno, J. Murota and S. Ono, *J. Crystal Growth* **115**, 439 (1991).
- ⁸S. Nakayama, I. Kawashima and J. Murota, *J. Electrochem. Soc.* **133**, 1721 (1986).
- ⁹C.P. Parry, S.M. Newstead, R.D. Barlow, P. Augustus, R.A. Kubiak, M.G. Dowsutt, T.E. Whall and E.H.C. Parker, *Appl. Phys. Lett.* **58**, 481 (1991).

- ¹⁰C.P. Parry, R.A. Kubiak, S.M. Newstead, T.E. Whall and E.H.C. Parker, *J. Appl. Phys.* **71**, 118 (1992).
- ¹¹B.S. Meyerson, F.K. LeGoues, T.N. Nguyen and D.L. Harame, *Appl. Phys. Lett.* **50**, 113 (1987).
- ¹²R.L. Headrick, B.E. Weir, A.F.J. Levi, D.J. Eaglesham and L.C. Feldman, *Appl. Phys. Lett.* **57**, 2779 (1990).
- ¹³R.L. Headrick, B.E. Weir, A.F.J. Levi, B. Freer, J. Bevk and L.C. Feldman, *J. Vac. Sci. Technol. A* **9**, 2269 (1991).
- ¹⁴R.L. Headrick, B.E. Weir, A.F.J. Levi, D.J. Eaglesham and L.C. Feldman, *J. Crystal Growth* **111**, 838 (1991).
- ¹⁵B.E. Weir, L.C. Feldman, D. Monroe, H.-J. Grossmann, R.L. Headrick and T.R. Hart, *Appl. Phys. Lett.* **65**, 737 (1994).
- ¹⁶B.E. Weir, R.L. Headrick, Q. Shen, L.C. Feldman, M.S. Hybertsen, M. Needels, M. Schluter and T.R. Hart, *Phys. Rev. B* **46**, 12861 (1992).
- ¹⁷Y. Wang, R.J. Hamers and E. Kaxiras, *Phys. Rev. Lett.* *In Press*, (1994).
- ¹⁸Y. Wang and R.J. Hamers, *J. Vac. Sci. Technol. A* *In Press*, (1994).
- ¹⁹G.L. Vick and K.M. Whittle, *J. Electrochem Soc.* **116**, 1142 (1969).
- ²⁰H.-N. Yang, A. Chan and G.-C. Wang, *J. Appl. Phys.* **74**, 101 (1993).
- ²¹W.M. Tong and R.S. Williams, *Ann. Rev. Phys. Chem.* 1994 **45**, 401 (1994).
- ²²P.D. Agnello, T.O. Sedgwick and J. Cotte, *J. Electrochem. Soc.* **140**, 2703 (1993).
- ²³H. Hirayama, M. Hiroi, K. Koyama and T. Tatsumi, *J. Crystal Growth* **111**, 856 (1991).

Figure Captions:

- 1a) STM image of boron-induced reconstructions on Si(001). Image dimensions 485 Å x 485 Å, -2V sample bias, 0.2 nA current.
- 1b) High-resolution image, 192 Å x 254 Å. Arrows point to individual unit cells of boron-induced reconstructions.
- 2) STM Images showing growth of disilane on clean and boron-exposed Si(001) surfaces, prepared as described in text.
- 2a) 2 monolayers Si on boron-exposed surface; 4700 Å x 2980 Å
- 2b) 10 monolayers Si on boron-exposed surface, 4700 Å x 2980 Å
- 2c) 10 monolayers Si on boron-exposed surface, 242 Å x 178 Å
- 2d) 10 monolayers Si on clean Si(001), 4700 Å x 2980 Å
- 3a) Surface height distributions measured on surfaces shown in fig. 2b and 2d.
- 3b) Height-height correlation function measured on surfaces shown in fig. 2b and 2d.



Wang and Hamers
Appl. Phys. Lett.
Figure 1

